

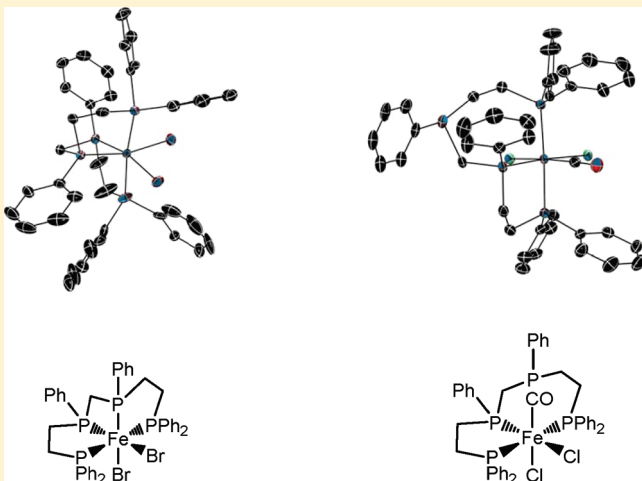
Synthesis of Monomeric Fe(II) and Ru(II) Complexes of Tetradentate Phosphines

Barun Jana, Arkady Ellern, Oleg Pestovsky,* Aaron Sadow,* and Andreja Bakac*

Ames Laboratory and Chemistry Department, Iowa State University, Ames, Iowa 50011, United States

Supporting Information

ABSTRACT: *rac*-Bis[{(diphenylphosphino)ethyl}-phenylphosphino]methane (DPPEPM) reacts with iron(II) and ruthenium(II) halides to generate complexes with folded DPPEPM coordination. The paramagnetic, five-coordinate Fe-(DPPEPM)Cl₂ (**1**) in CD₂Cl₂ features a tridentate binding mode as established by ³¹P{¹H} NMR spectroscopy. Crystal structure analysis of the analogous bromo complex, Fe-(DPPEPM)Br₂ (**2**) revealed a pseudo-octahedral, *cis*-α geometry at iron with DPPEPM coordinated in a tetradentate fashion. However, in CD₂Cl₂ solution, the coordination of DPPEPM in **2** is similar to that of **1** in that one of the external phosphorus atoms is dissociated resulting in a mixture of three tridentate complexes. The chloro ruthenium complex *cis*-Ru-(κ⁴-DPPEPM)Cl₂ (**3**) is obtained from *rac*-DPPEPM and either [RuCl₂(COD)]₂ [COD = 1,5-cyclooctadiene] or RuCl₂(PPh₃)₄. The structure of **3** in both the solid state and in CD₂Cl₂ solution features a folded κ⁴-DPPEPM. This binding mode was also observed in *cis*-[Fe(κ⁴-DPPEPM)(CH₃CN)₂](CF₃SO₃)₂ (**4**). Addition of an excess of CO to a methanolic solution of **1** results in the replacement of one of the chloride ions by CO to yield *cis*-[Fe(κ⁴-DPPEPM)Cl(CO)](Cl) (**5**). The same reaction in CH₂Cl₂ produces a mixture of **5** and [Fe(κ³-DPPEPM)Cl₂(CO)] (**6**) in which one of the internal phosphines has been substituted by CO. Complexes **2**, **3**, **4**, and **5** appear to be the first structurally characterized monometallic complexes of κ⁴-DPPEPM.



INTRODUCTION

Multidentate ligands are often used to provide stabilized coordination complexes through the chelate effect. At the same time, the structure of a polydentate ligand provides means to control the bite angle, chelate ring size, and stereochemistry. The resulting electronic and steric effects can be used to enhance the reactivity of a metal center. In well-studied organometallic examples, ansa-metalloenes^{1–3} and constrained-geometry compounds^{4–9} provide enhanced reactivity in olefin polymerization and bond activation, while inhibiting disproportionation reactions. Similarly, bidentate phosphines enforce *cis* coordination geometries, even though *trans* configurations might be sterically or electronically preferred, and tridentate phosphines such as MeSi(CH₂PMe₂)₃^{10–12} and [PhB(CH₂PⁱPr₂)₃]^{13,14} enforce fac-coordination modes. Branched tetradentate ligands, such as P(CH₂CH₂PR₂)₃^{15,16} and P(CH₂CH₂CH₂PMe₂)₃,^{17–19} are constrained to keep the nonphosphine “reactive” coordination sites disposed *cis*.

Linear tetradentate ligands can coordinate in several configurations, including *trans*, *cis*-α, and *cis*-β.²⁰ Notably, the linear, ethylene-bridged, tetraphosphine ligand Ph₂CH₂CH₂PPhCH₂CH₂PPhCH₂CH₂PPh₂ (DPPEPE, Chart 1) typically provides

trans compounds with Group 8 metal centers^{21,22} with structures similar to those of complexes with two bidentate ligands such as *trans*-FeCl₂(dmpe)₂ (dmpe = bis(dimethylphosphino)ethane,²³ [FeH(H₂)(dmpe)₂][BPh₄]²⁴ and FeCl₂(DHPePE)₂ (DHPePE = 1,2-bis(bis(hydroxypropyl)phosphino)ethane).²⁵ The *trans* geometry in these compounds may limit their reactivity by suppressing processes that require *cis*-disposed valencies, although *cis*-iron(II) complexes of bidentate and meso isomers of linear tetradentate phosphines are also formed on occasion.^{23,25–30}

Ligand modifications can introduce strain, as well as control the geometry and configuration of late metal polyphosphine complexes. One approach involves replacing the central ethylene unit in DPPEPE with a methylene to shorten the ligand backbone and provide the ligand Ph₂PCH₂CH₂PPhCH₂CH₂PPhCH₂CH₂PPh₂ (DPPEPM, Chart 1).³¹ Monometallic rhodium(III) compounds of the related tetraphosphine-containing diethylphosphino groups, Et₂PCH₂CH₂PPhCH₂CH₂PPhCH₂CH₂PEt₂ (DEPEPM), have been reported. The configuration of

Received: December 15, 2010

Published: March 07, 2011

$[(\text{DEPEPM})\text{RhCl}_2]^+$ and $[(\text{DEPEPM})\text{RhCl}(\text{CH}_2\text{Cl})]^+$ is *cis- α* .³² Palladium and platinum compounds of the perphenylated DPPEPM, on the other hand, are typically bimetallic,³³ although monometallic complexes containing κ^2 - or κ^3 -DPPEPM can also be obtained under appropriate conditions.³⁴ In group 8 chemistry, a related hexaphosphine ligand $(\text{Et}_2\text{PCH}_2\text{CH}_2)_2\text{-PCH}_2\text{P}(\text{CH}_2\text{CH}_2\text{PEt}_2)_2$ (eHTP) coordinates in a tetradentate, *cis- α* configuration to Fe(II).³⁵ Bis(diphospholanylethane) iron(II) chloride $[(\text{BPES})_2\text{FeCl}_2]$ adopts a *cis- α* geometry presumably for steric reasons,²⁶ while $\kappa^4\text{-}\{\text{P}(\text{CH}_2\text{CH}_2\text{PMe}_2)_3\}\text{FeX}_2$ gives *cis*-complexes because of the connectivity of the ancillary ligand.^{15,16}

Our interest in phosphine complexes of group 8 metals arises from their potential in nitrogen activation and reduction.^{22,24,36} In a recent example, an iron complex containing two bidentate phosphine ligands has been shown to react with molecular hydrogen and nitrogen through a series of intermediates to generate measurable amounts of ammonia and hydrazine.³⁶ On the basis of the few examples described above, we expected that a complex with a tetradentate P_4 ligand, such as DPPEPM, forced

by its short backbone into folded geometry, should be more efficient in enabling monometallic reactivity by positioning the substrate and reactants adjacent (*cis*) to each other.

The goal of this study was to synthesize iron(II) and ruthenium(II) complexes of DPPEPM, establish expected coordination modes, and identify substitution pathways to examine the potential of such complexes in various catalytic reactions, including reduction of nitrogen. Even though DPPEPM has been known for several decades, group 8 metal complexes of this ligand have not previously been reported. Herein, we describe the synthesis, spectroscopic and structural characterization, and reactivity of several DPPEPM coordination complexes.

EXPERIMENTAL SECTION

All the reactions and manipulations were performed under a dry nitrogen atmosphere in a glovebox or on a Schlenk line. Methylene chloride, toluene, pentane, diethyl ether, and tetrahydrofuran were dried and deoxygenated in an IT PureSolv system. Acetone was used immediately after distillation. Tetrahydrofuran- d_8 was heated to reflux over Na/K alloy and vacuum-transferred. CD_2Cl_2 was heated to reflux over CaH_2 and vacuum-transferred. CD_3OD was distilled and was stored over molecular sieves.

The ligand DPPEPM was obtained as a mixture of isomers in 90% yield by a literature procedure.³¹ The *meso* and *rac* diastereomers were separated by fractional crystallization from ether. The *meso* form precipitated first as a white powder and was separated by filtration. The mother liquor was evaporated to dryness, and the sticky, colorless

Chart 1

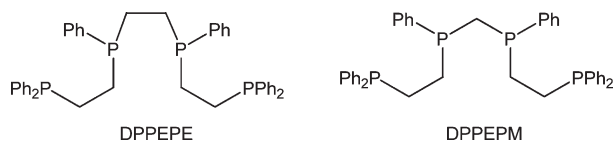


Table 1. ^1H NMR and $^{31}\text{P}\{^1\text{H}\}$ NMR Data and CO/CF Stretching Frequencies of the Reported Compounds^a

compounds	solvent: ^1H NMR, ppm	solvent: $^{31}\text{P}\{^1\text{H}\}$, ppm	IR, cm^{-1}
<i>rac</i> -DPPEPM ³¹	CD_3OD : 1.82–2.00, 2.01–2.13, 2.14–2.22 ($\text{P-CH}_2\text{-CH}_2\text{-P}$); 2.25 (t, $\text{P-CH}_2\text{-P}$)	C_6D_6 : –25.8 (1 P_{int} dd); –25.2 (1 P_{int} dd); –11.9 (2 P_{ext} dd)	
$\text{Fe}(\text{DPPEPM})\text{Cl}_2$ (1)	CD_2Cl_2 : –3.20 (br), –0.7 to 1.34 (br), 3.21–4.02 (br), 6.25–9.41 (br), 11.09 (br), 13.60 (br)	CD_2Cl_2 : –9.2 (br), 8.9 (br), 16.0 (br), 53.4 (br) THF- d_8 : –2.7 (br), 7.4 (br), 15.8 (br), 54.8 (br), 58.8 (br) CD_3CN : 45.2 (2P, t, $^2J_{\text{PP}}$ 35 Hz), 72.3 (2P, t, $^2J_{\text{PP}}$ 35 Hz)	
$\text{Fe}(\text{DPPEPM})\text{Br}_2$ (2)	CD_2Cl_2 : 2.3 (br), 3.1 (br), 3.3 (br), 3.5 (br), 3.75 (br), 6.76 (m), 6.95 (m), 7.16 (m), 7.33 (m), 7.47 (m), 8.27 (m)	CD_2Cl_2 : –1.9 (br), 8.8 (br), 14.8 (br), 51.8 (br), 56.9 (br), 65.2 (br)	
$\text{Ru}(\text{DPPEPM})\text{Cl}_2$ (3)	CD_2Cl_2 : 2.17 (m, $\text{PCH}_2\text{CH}_2\text{P}$), 2.36 (m, $\text{PCH}_2\text{CH}_2\text{P}$), 2.95 (m, $\text{PCH}_2\text{CH}_2\text{P}$), 3.90 (m, PCH_2P), 6.80–8.00 (PPh)	CD_2Cl_2 : 27.8 (2P, t, $^2J_{\text{PP}}$ 19 Hz), 47.6 (2P, t, $^2J_{\text{PP}}$ 19 Hz)	
$[\text{Fe}(\text{DPPEPM})(\text{CH}_3\text{CN})_2](\text{OTf})_2$ (4)	CD_2Cl_2 : 2.02 (s, CH_3CN), 2.20 (m, $\text{PCH}_2\text{CH}_2\text{P}$), 2.60 (m, $\text{PCH}_2\text{CH}_2\text{P}$), 2.96 (m, $\text{PCH}_2\text{CH}_2\text{P}$), 3.44 (m, $\text{PCH}_2\text{CH}_2\text{P}$), 4.13 (t, PCH_2P), 6.98–7.85 (m, PPh)	CD_2Cl_2 : 42.8 (2P, t, $^2J_{\text{PP}}$ 35 Hz), 69.7 (2P, t, $^2J_{\text{PP}}$ 35 Hz)	$\nu_{\text{C-F}} = 1209$
$[\text{Fe}(\text{DPPEPM})\text{Cl}(\text{CO})](\text{Cl})$ (5)	CD_3OD : 2.17–2.30 (br m, $\text{PCH}_2\text{CH}_2\text{P}$), 2.56–2.82 (br m, $\text{PCH}_2\text{CH}_2\text{P}$), 2.88–3.25 (br m, $\text{PCH}_2\text{CH}_2\text{P}$), 3.30 (br m, ($\text{PCH}_2\text{CH}_2\text{P}$ and PCH_2P), 6.91 (m, Ph), 7.12 (m, Ph), 7.14 (m, Ph), 7.20–7.40 (m, Ph), 7.43 (m, Ph), 7.56 (m, Ph), 7.91 (m, Ph), 8.15 (m, Ph)	CD_3OD : 26.7, 52.3, 61.8, 85.3 (all four P ddd, $^2J_{\text{PP}} = 117, 115, 48, 31, 26, 22$ Hz)	$\nu_{\text{C=O}} = 1942$
$\text{Fe}(\text{DPPEPM})\text{Cl}_2(\text{CO})$ (6)	CD_2Cl_2 : 1.27–2.98 (br, $\text{PCH}_2\text{CH}_2\text{P}$ and PCH_2P), 7.00–8.17 (m, PPh)	CD_2Cl_2 : –11.5 (br, uncoordinated P), 20.9 (m), 28.4 (m), 53.2 (m), 55.2 (m), 63.7 (m), 77.2 (m), 87.2 (m)	$\nu_{\text{C=O}} = 1955$

^a Abbreviations: m = multiplet, s = singlet, d = doublet, t = triplet, br = broad.

residue was heated under vacuum at 200 °C for two hours to yield *rac*-DPPEPM in 70% yield. ^1H and $^{31}\text{P}\{^1\text{H}\}$ NMR data agreed well with the literature values³¹ and are presented in Table 1.

Anhydrous FeCl_2 (Strem) and FeBr_2 (Sigma-Aldrich) were used as received. $\text{Fe}(\text{CH}_3\text{CN})_2(\text{OTf})_2$,³⁷ $\text{Ru}(\text{COD})\text{Cl}_2$,³⁸ and $\text{Ru}(\text{PPh}_3)_3\text{Cl}_2$ ³⁹ were synthesized by literature procedures. Elemental analyses were performed with a Perkin-Elmer 2400 Series II CHN/S by the Iowa State Chemical Instrumentation Facility. X-ray diffraction data were collected with a Bruker-AXS SMART 1000 CCD diffractometer using Bruker-AXS SHELXTL software. ^1H NMR, $^{31}\text{P}\{^1\text{H}\}$ NMR, and ^{19}F NMR spectra were recorded with a Bruker 400 spectrometer. ^1H NMR spectra of the paramagnetic **1**, and $^{31}\text{P}\{^1\text{H}\}$ NMR spectra of **2** were collected with a relaxation delay of 130 ms to improve signal-to-noise ratio. Spectra obtained with the more standard relaxation delay of one second appeared to be identical but required much longer acquisition times for the same S/N ratio. The signals in the ^1H NMR spectrum of **5** were broad, but a reasonably sharp $^{31}\text{P}\{^1\text{H}\}$ NMR spectrum was obtained. Paramagnetism of **1** and **2** was confirmed by the Evans method,⁴⁰ 3.6 and 2.1 unpaired electrons for **1** and **2**, respectively.

Synthesis of $\text{Fe}(\text{DPPEPM})\text{Cl}_2$ (1**).** A solution of 1.17 g (1.78 mmol) of *rac*-DPPEPM in 40 mL of CH_2Cl_2 was stirred in a 250 mL Schenk round-bottom flask for 10 min at room temperature. Solid FeCl_2 (0.226 g, 1.78 mmol) was slowly added at ambient temperature. The resulting mixture was stirred for 8 h, after which time the solvent was removed under reduced pressure. The violet solid product was washed with 30 mL of pentane, diethyl ether (2×20 mL), and dried under vacuum. Yield: 1.12 g (1.32 mmol, 80%). ^1H NMR (400 MHz, CD_2Cl_2): δ -3.20 (br), -0.7 to 1.34 (br), 3.21–4.02 (br), 6.25–9.41 (br), 11.09 (br), 13.60 (br). $^{31}\text{P}\{^1\text{H}\}$ NMR (CD_2Cl_2 , 162 MHz): δ -9.2 (br), 8.9 (br), 16.0 (br), 53.4 (br). $^{31}\text{P}\{^1\text{H}\}$ NMR ($\text{THF}-d_8$, 162 MHz): δ -2.7 (br), 7.4 (br), 15.8 (br), 54.8 (br), 58.8 (br). $^{31}\text{P}\{^1\text{H}\}$ NMR (CD_3CN , 162 MHz): δ 45.2 (2P, t, $^2J_{\text{PP}}$ 35 Hz), 72.3 (2P, t, $^2J_{\text{PP}}$ 35 Hz). ESI-MS: 782 (M^+), 747 ($\text{M}^+ - \text{Cl}$). IR (KBr, cm^{-1}): 808 (w), 873 (w), 913 (w), 999 (w), 1026 (w), 1068 (w), 1097 (m), 1159 (w), 1180 (w), 1272 (w), 1310 (w), 1331 (w), 1433 (s), 1482 (m), 1571 (w), 1585 (w), 1659 (w), 1815 (w), 1890 (w), 1963 (w), 2908 (w), 2960 (w), 3002 (w), 3057 (m). Anal. Calcd for $\text{C}_{41}\text{H}_{40}\text{P}_4\text{Cl}_2\text{Fe}$: C 62.86, H 5.15; Found C 62.49, H 5.01. mp: 117–121 °C.

Synthesis of $\text{Fe}(\text{DPPEPM})\text{Br}_2$ (2**).** *rac*-DPPEPM (0.27 g, 0.40 mmol) was dissolved in 15 mL of THF. Solid FeBr_2 (0.087 g, 0.40 mmol) was added at room temperature. The reaction mixture was stirred for 8 h during which time the color changed from light green to purple and then to gray. After evaporation of the solvent, the dark gray residue was washed with diethyl ether (2×10 mL) and dried under vacuum for 2 h. Yield: 0.290 g (3.3 mmol; 82%). Single crystals suitable for X-ray diffraction were obtained from a concentrated THF solution at room temperature over two days. ^1H NMR (CD_2Cl_2 , 400 MHz): δ 2.3 (br), 3.1 (br), 3.3 (br), 3.5 (br), 3.75 (br), 6.76 (m), 6.95 (m), 7.16 (m), 7.33 (m), 7.47 (m), 8.27 (m). $^{31}\text{P}\{^1\text{H}\}$ NMR (CD_2Cl_2): δ -1.9 (br), 8.8 (br), 14.8 (br), 51.8 (br), 56.9 (br), 65.2 (br). IR (KBr, cm^{-1}): 818 (w), 880 (w), 999 (w), 1028 (w), 1071 (w), 1094 (m), 1159 (w), 1188 (w), 1262 (w), 1314 (w), 1410 (w), 1433 (s), 1482 (m), 1584 (w), 2920 (w), 2949 (w), 3057 (m). Anal. Calcd for $\text{C}_{41}\text{H}_{40}\text{P}_4\text{Br}_2\text{Fe}$: C 56.45, H 4.62; Found C, 56.18; H, 4.72. mp: 202–206 °C.

Synthesis of $\text{Ru}(\text{DPPEPM})\text{Cl}_2$ (3**).** *Method 1.* DPPEPM (0.216 g, 0.33 mmol), dissolved in 10 mL of CH_2Cl_2 , was added dropwise to a suspension of $\text{RuCl}_2(\text{PPh}_3)_4$ (0.402 g, 0.33 mmol) in CH_2Cl_2 . The solution turned yellow. After the mixture was stirred for 8 h, the solvent was removed under reduced pressure to give a light yellow solid that was washed with 10 mL of pentane, diethyl ether (2×20 mL), and dried under vacuum. Yield: 0.22 g (0.27 mmol; 81%).

Method 2. A solution of DPPEPM (0.54 g, 0.82 mmol), dissolved in 15 mL of CH_2Cl_2 , was added dropwise to a suspension of $[\text{Ru}(\text{COD})\text{Cl}_2]_2$ (0.230 g, 0.82 mmol) in 10 mL of CH_2Cl_2 over 5 min at

room temperature. The reaction mixture was heated at 60 °C until the color turned dark yellow. The solvent was removed under reduced pressure to give a yellow solid. That solid was washed with 10 mL of dry pentane, diethyl ether (2×10 mL), and dried under vacuum. Yield: 0.60 g (0.72 mmol, 89%). ^1H NMR (CD_2Cl_2 , 400 MHz): δ 2.17 (m, $\text{PCH}_2\text{CH}_2\text{P}$), 2.36 (m, $\text{PCH}_2\text{CH}_2\text{P}$), 2.95 (m, $\text{PCH}_2\text{CH}_2\text{P}$), 3.90 (m, PCH_2P), 6.80–8.00 (PPh). $^{31}\text{P}\{^1\text{H}\}$ NMR (CD_2Cl_2 , 162 MHz): δ 27.8 (2P, t, $^2J_{\text{PP}}$ 19 Hz), 47.6 (2P, t, $^2J_{\text{PP}}$ 19 Hz). IR (KBr, cm^{-1}): 819 (w), 880 (w), 999 (w), 1028 (w), 1098 (m), 1158 (w), 1189 (w), 1262 (w), 1336 (w), 1409 (w), 1433 (s), 1484 (m), 1570 (w), 1585 (w), 3000 (w), 3074 (m). Anal. Calcd for $\text{C}_{41}\text{H}_{40}\text{P}_4\text{Cl}_2\text{Ru}$: C 59.43, H 4.87; Found C 59.62, H 4.75. mp: 194–196 °C.

Synthesis of $[\text{Fe}(\text{DPPEPM})(\text{CH}_3\text{CN})_2](\text{OTf})_2$ (4**).** DPPEPM (0.54 g, 0.822 mmol) in 15 mL of CH_2Cl_2 was added dropwise to a solution of $\text{Fe}(\text{CH}_3\text{CN})_2(\text{OTf})_2$ (0.25 g, 0.822 mmol) in 5 mL of CH_2Cl_2 at ambient temperature. The resulting reddish-orange solution was allowed to stir for 14 h. After the removal of solvent under vacuum, the reddish-orange residue was washed with 10 mL of pentane, 10 mL of diethyl ether, and dried under vacuum. Yield: 0.76 g (0.68 mmol, 82%). X-ray quality crystals were obtained from a concentrated acetone solution at room temperature after 2 d. ^1H NMR (CD_2Cl_2 , 400 MHz): δ 2.02 (5.6 H s, CH_3CN), 2.20 (2.1 H m, $\text{PCH}_2\text{CH}_2\text{P}$), 2.60 (2.0 H m, $\text{PCH}_2\text{CH}_2\text{P}$), 2.96 (2.0 H m, $\text{PCH}_2\text{CH}_2\text{P}$), 3.44 (1.9 H m, $\text{PCH}_2\text{CH}_2\text{P}$), 4.13 (1.8 H t, PCH_2P , $^2J_{\text{PH}}$ 12 Hz), 6.98–7.85 (30.8 H m, PPh). $^{31}\text{P}\{^1\text{H}\}$ NMR (CD_2Cl_2 , 162 MHz): δ 42.8 (2P, t, $^2J_{\text{PP}}$ 35 Hz), 69.7 (2P, t, $^2J_{\text{PP}}$ 35 Hz). ^{19}F NMR (CD_2Cl_2 , 376 MHz): δ -77.4 (OSO_2CF_3). IR (KBr, cm^{-1}): 813 (w), 873 (w), 999 (w), 1209 (triflate), 1099 (m), 1152 (s), 1223 (m), 1260 (vs, triflate), 1368 (w), 1483 (m), 1585 (w), 1658 (w, CN), 2922 (w), 2966 (m), 3053 (s). Anal. Calcd for $\text{C}_{47}\text{H}_{46}\text{F}_6\text{N}_2\text{O}_8\text{P}_4\text{S}_2\text{Fe}$: C 51.66, H 4.24, N 2.56; Found C 51.49, H 3.98, N 2.46. mp: 105–107 °C.

Synthesis of $[\text{Fe}(\text{DPPEPM})(\text{Cl})(\text{CO})]\text{Cl}$ (5**).** A violet solution of $\text{Fe}(\text{DPPEPM})\text{Cl}_2$ (0.237 g, 0.30 mmol) in 25 mL of CH_3OH was degassed with three freeze–pump–thaw cycles. The solution was frozen in a liquid nitrogen bath, and the headspace was charged with carbon monoxide (1 atm). The flask was sealed, and the reaction mixture was allowed to warm to room temperature and was stirred for 24 h, over which time the color changed from violet to orange. The solvent was removed under reduced pressure, and the orange residue was washed with diethyl ether (2×10 mL) and dried. Crystals for structural analysis were grown from methanol at 0 °C. Yield: 0.16 g (67%). ^1H NMR (CD_3OD , 400 MHz): δ 2.17–2.30 (br m, $\text{PCH}_2\text{CH}_2\text{P}$), 2.56–2.82 (br m, $\text{PCH}_2\text{CH}_2\text{P}$), 2.88–3.25 (br m, $\text{PCH}_2\text{CH}_2\text{P}$), 3.30 (br m, ($\text{PCH}_2\text{CH}_2\text{P}$ and PCH_2P), 6.91 (m, Ph), 7.12 (m, Ph), 7.14 (m, Ph), 7.20–7.40 (m, Ph), 7.43 (m, Ph), 7.56 (m, Ph), 7.91 (m, Ph), 8.15 (m, Ph). $^{31}\text{P}\{^1\text{H}\}$ NMR (CD_3OD , 162 MHz): δ 26.7, 52.3, 61.8, 85.3 (all four P ddd, $^2J_{\text{PP}}$ = 117, 115, 48, 31, 26, 22 Hz). IR (KBr, cm^{-1}): 798 (w), 877 (w), 998 (w), 1026 (vs), 1103 (m), 1159 (w), 1188 (w), 1269 (w), 1311 (w), 1433 (s), 1482 (m), 1584 (w), 1942 (vs, CO), 2827 (w), 2903 (w), 2941 (w), 3077 (s). Anal. Calcd for $\text{C}_{42}\text{H}_{40}\text{OP}_4\text{Cl}_2\text{Fe}$: C 62.17, H 4.97; Found C 62.49, H 5.01. mp: 219–222 °C.

Synthesis of $\text{Fe}[(\text{DPPEPM})\text{Cl}_2(\text{CO})]$ (6**).** $\text{Fe}(\text{DPPEPM})\text{Cl}_2$ (0.167 g; 0.21 mmol) was dissolved in 15 mL of CH_2Cl_2 in a 100 mL Schlenk flask. The violet solution was degassed with three freeze–pump–thaw cycles and charged with one atmosphere of carbon monoxide at liquid nitrogen temperature. The sealed solution was allowed to warm to room temperature and was stirred for 24 h. During this time, the color of the solution changed from violet to yellow. The solvent was removed under reduced pressure, and the yellow residue was washed with 2×10 mL of diethyl ether. Single crystals for X-ray crystal structure determination were obtained by dissolving the residue in 20 mL of CH_2Cl_2 and placing the solution in a freezer at -30 °C. The crystals formed within several days. Yield: 0.15 g (0.18 mmol, 87%).

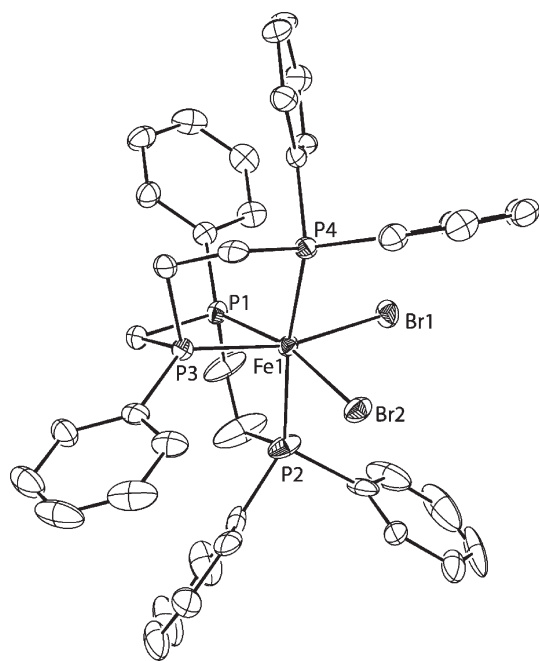


Figure 1. ORTEP drawing of $\text{Fe}(\text{DPPEPM})\text{Br}_2$ (**2**). Thermal ellipsoids are drawn at 35% probability level. Two molecules of $\text{FeBr}_2(\text{DPPEPM})$ are found in a unit cell, and both possess identical connectivity and similar bond lengths and angles. One molecule and the hydrogen atoms are omitted for clarity. Selected bond lengths [Å] and angles [deg]: $\text{Br1}-\text{Fe1}$ 2.5149(7), $\text{Br2}-\text{Fe1}$ 2.5054(7), $\text{Fe1}-\text{P3}$ 2.1939(13), $\text{Fe1}-\text{P1}$ 2.2092(12), $\text{Fe1}-\text{P2}$ 2.2897(14), $\text{Fe1}-\text{P4}$ 2.3204(13), $\text{P3}-\text{Fe1}-\text{P1}$ 73.12(5), $\text{P3}-\text{Fe1}-\text{P2}$ 98.36(5), $\text{P1}-\text{Fe1}-\text{P2}$ 83.80(5), $\text{P3}-\text{Fe1}-\text{P4}$ 85.29(5), $\text{P1}-\text{Fe1}-\text{P4}$ 105.80(5), $\text{P2}-\text{Fe1}-\text{P4}$ 170.38(5), $\text{P3}-\text{Fe1}-\text{Br2}$ 100.08(4), $\text{P1}-\text{Fe1}-\text{Br2}$ 167.72(4), $\text{P2}-\text{Fe1}-\text{Br2}$ 87.19(4), $\text{P4}-\text{Fe1}-\text{Br2}$ 83.39(4), $\text{P3}-\text{Fe1}-\text{Br1}$ 162.52(4), $\text{P1}-\text{Fe1}-\text{Br1}$ 91.52(4), $\text{P2}-\text{Fe1}-\text{Br1}$ 87.95(4), $\text{P4}-\text{Fe1}-\text{Br1}$ 91.13(4), $\text{Br2}-\text{Fe1}-\text{Br1}$ 96.48(3).

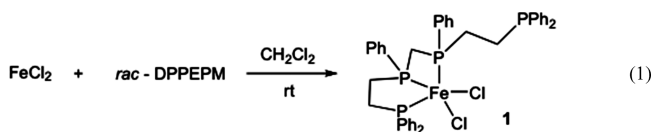
^1H NMR (CD_2Cl_2 , 400 MHz): δ 1.27–2.98 (br, $\text{PCH}_2\text{CH}_2\text{P}$ and PCH_2P), 7.00–8.17 (m, PPh). $^{31}\text{P}\{^1\text{H}\}$ NMR (CD_2Cl_2 , 162 MHz): δ –11.5 (br, noncoordinated P), 20.9 (m), 28.4 (m), 53.2 (m), 55.2 (m), 63.7 (m), 77.2 (m), 87.2 (m). IR (KBr, cm^{-1}): 806 (w), 869 (w), 999 (w), 1026 (vs), 1099 (m), 1159 (w), 1189 (w), 1255 (w), 1309 (w), 1434 (s), 1484 (m), 1585 (w), 1955 (vs, CO), 2913 (w), 2964 (w), 3053 (s). Anal. Calcd for $\text{C}_{42}\text{H}_{40}\text{OP}_4\text{Cl}_2\text{Fe}$: C 62.09, H 5.09; Found C 61.17, H 5.16. mp: $>300^\circ\text{C}$. The 2% discrepancy between the experimental and calculated values of carbon content is likely caused by the instability of the complex.

RESULTS AND DISCUSSION

Synthesis and Characterization. To facilitate the formation of *cis-α* metal complexes, we focused on the racemic diastereomer of the ligand. Work with related rhodium complexes³² has shown that coordination of the meso form generates a less stable complex because of unfavorable steric factors.

The reaction of *rac*-DPPEPM with one equivalent of FeCl_2 in methylene chloride at room temperature, eq 1, yielded $\text{Fe}(\kappa^3\text{-DPPEPM})\text{Cl}_2$ (**1**) in 80% yield. Compound **1** is air sensitive and soluble in CH_2Cl_2 , alcohols and THF, but insoluble in benzene, pentane, and toluene. The ESI-MS spectrum of a solution in CH_2Cl_2 shows the molecular ion peak at m/z 782 (M^+) and base

peak at 747 ($\text{M}^+ - \text{Cl}$). Attempts to obtain an X-ray quality single crystal of **1** were not successful.



Violet solutions of **1** in CD_2Cl_2 exhibit four broad resonances in the $^{31}\text{P}\{^1\text{H}\}$ NMR spectrum (CD_2Cl_2) at –9.2, 8.9, 16.0, and 53.4 ppm, Table 1. (Additional spectroscopic and structural information for the complexes presented in this work are given in the Supporting Information). This pattern is indicative of tridentate DPPEPM coordination.^{31,35,41} The signal at –9.2 ppm is close to that for the PPh_2 groups in the free ligand³¹ (–11.9 ppm, see Table 1) and is assigned to an uncoordinated external PPh_2 group in the complex. The resonances at 8.9 and 16.0 ppm correspond to the internal PPh_2 groups and that at 53.4 ppm to a coordinated external PPh_2 .

THF solutions of **1** are red and exhibit a $^{31}\text{P}\{^1\text{H}\}$ NMR ($\text{THF}-d_8$) spectrum similar to that in CD_2Cl_2 , except that there are now two downfield resonances corresponding to coordinated PPh_2 . This pattern is consistent with a mixture of two complexes, where the second complex likely contains a coordinated THF molecule.

The complex $\text{Fe}(\text{DPPEPM})\text{Br}_2$ (**2**) was synthesized from FeBr_2 and one equivalent of *rac*-DPPEPM in THF at room temperature. The compound was isolated as a dark-gray solid that was poorly soluble in THF and moderately soluble in CH_2Cl_2 . A single crystal X-ray diffraction analysis revealed four phosphorus atoms and two bromide ions coordinated in a pseudo-octahedral, *cis-α* conformation, Figure 1. Both bromide ions are *trans* to the internal phosphorus atoms. In this compound, and in all of the κ^4 -DPPEPM complexes described in this work, the $\text{Fe}-\text{P}$ (internal) bonds are somewhat shorter than $\text{Fe}-\text{P}$ (external) bonds. In particular, the $\text{Fe1}-\text{P1}$ and $\text{Fe1}-\text{P3}$ bonds lengths in the PhPCH_2PPh moiety are 2.209(1) and 2.194(1) Å, whereas $\text{Fe1}-\text{P2}$ and $\text{Fe1}-\text{P4}$ distances are 2.290(1) and 2.320(1) Å. This is believed to be a result of the elongation and bending of $\text{Fe}-\text{P}$ (external) bonds to reduce the overall strain, but this motion pulls the internal phosphines closer to the metal. The weaker *trans* influence of bromide in comparison to a diarylalkylphosphine may also favor shorter $\text{Fe}-\text{P}$ (internal) distances, as was reported for the *cis*-dichloro complexes (BPES)₂- FeCl_2 and $\text{P}(\text{CH}_2\text{CH}_2\text{PMe}_2)_3\text{FeCl}_2$ complexes.^{17,26}

In contrast to the solid state structure, **2** appears to have the P_4 ligand bound in a κ^3 mode in CD_2Cl_2 solution, as judged by $^{31}\text{P}\{^1\text{H}\}$ NMR spectrum, which exhibits features similar to those of the dichloro compound. Specifically, the resonance in the negative range, –1.9 ppm, is indicative of an uncoordinated external PPh_2 group. Also, two resonances are present in the low field range, and a third one grows in at 56.9 ppm over time (approximately 10 min at room temperature), indicating that yet another form is generated. Despite the complexity of the $^{31}\text{P}\{^1\text{H}\}$ NMR spectra of **2**, analytical data confirm that its constitution is identical to that of the crystals characterized by X-ray diffraction.

The interpretation of the NMR spectra of compounds **1** and **2** is further complicated by their paramagnetic natures (in contrast, a related tetradentate phosphine complex FeL_4Cl_2 bearing a self-assembled phosphine is diamagnetic)⁴² and the difference between solution and solid state structures. To better assess the solution structures of these compounds, we sought a ruthenium

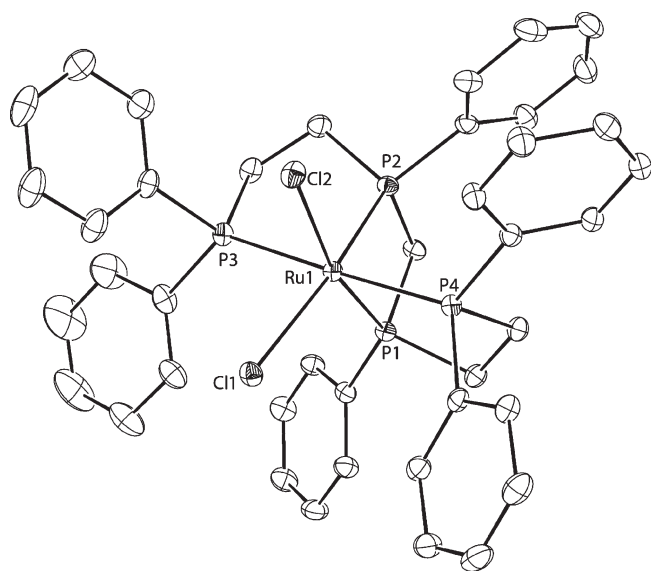
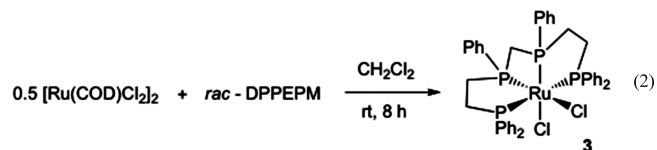


Figure 2. ORTEP drawing of $\text{Ru}(\kappa^4\text{-DPPEPM})\text{Cl}_2$ (**3**). Thermal ellipsoids are drawn at 35% probability level. Two molecules of CH_2Cl_2 and hydrogen atoms are omitted for clarity. Selected bond lengths [Å] and angles [deg]: Ru1–P2 2.2489(5), Ru1–P1 2.2657(5), Ru1–P3 2.3564(5), Ru1–P4 2.3650(5), Ru1–Cl2 2.4658(5), Ru1–Cl1 2.4885(5), P2–Ru1–P1 72.12(2), P2–Ru1–P3 83.90(2), P1–Ru1–P3 96.81(2), P2–Ru1–P4 94.29(2), P1–Ru1–P4 83.607(2), P3–Ru1–P4 177.91(2), P2–Ru1–Cl2 95.17(2), P1–Ru1–Cl2 166.39(2), P3–Ru1–Cl2 86.375(2), P4–Ru1–Cl2 92.745(2), P2–Ru1–Cl1 170.05(2), P1–Ru1–Cl1 104.510(2), P3–Ru1–Cl1 87.270(2), P4–Ru1–Cl1 94.614(2), Cl2–Ru1–Cl1 88.824(2).

analog as a less labile, diamagnetic derivative. $\text{Ru}(\text{DPPEPM})\text{Cl}_2$ (**3**) was prepared from *rac*-DPPEPM and either $\text{RuCl}_2(\text{PPh}_3)_4$ or $[\text{RuCl}_2(\text{COD})]_2$. The latter reaction is shown in eq 2. The light-yellow, air-sensitive solid is soluble in THF and CH_2Cl_2 . There are five well-separated, broad signals of equal intensity in the ^1H NMR spectrum corresponding to five types of methylenic protons. The diamagnetic $^{31}\text{P}\{^1\text{H}\}$ NMR spectrum in CD_2Cl_2 shows two triplets at 27.8 and 47.6 ppm corresponding to two internal and two external phosphorus atoms, respectively.



The solid-state structure of **3** contains the DPPEPM ligand coordinated to ruthenium in a tetradentate *cis-α* geometry as in **2** (Figure 2). As in the iron DPPEPM complex, the internal Ru–P distances that are trans to chloride are shorter than the external ones. In contrast to **2**, however, the solid-state geometry of **3** is consistent with the solution-state structure suggested by $^{31}\text{P}\{^1\text{H}\}$ NMR spectroscopy.

The reaction between $\text{Fe}(\text{CH}_3\text{CN})_2(\text{OTf})_2$ and DPPEPM might have been expected to generate a product with reduced coordination number because steric constraints should make it difficult for two triflate anions to bind *cis* to each other and because the labile triflate and acetonitrile ligands could readily dissociate. We anticipated that a five-coordinate iron center containing an outer-sphere triflate would have different substitution chemistry than **1**. Contrary to this reasoning, the reddish-orange product contains

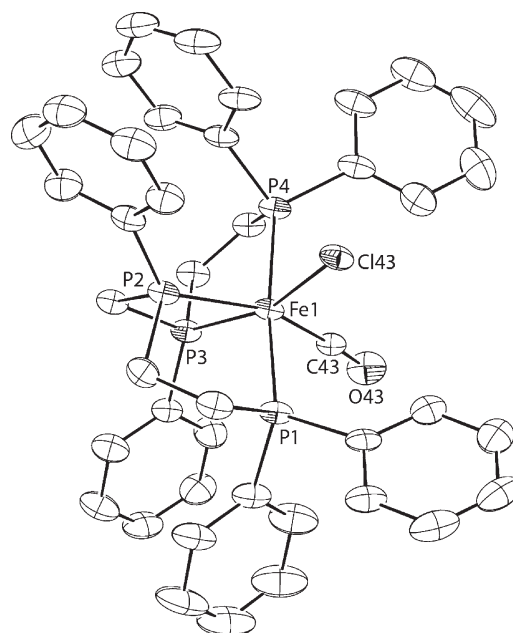


Figure 3. ORTEP drawing of the cationic portion $[\text{Fe}(\kappa^4\text{-DPPEPM})\text{-(Cl)(CO)}]\text{Cl}$ (**5**). Thermal ellipsoids are drawn at 35% probability level. Hydrogen atoms, two chloride counterions, and two molecules of methanol (crystallization solvent) are not shown. Selected bond lengths [Å] and angles [deg]: Fe1–C42 1.800(3), Fe1–P3 2.2389(1), Fe1–P4 2.2458(1), Fe1–P1 2.262(1), Fe1–P2 2.2626(2), Fe1–Cl42 2.312(5), C42–Fe1–P3 163.1(7), C42–Fe1–P4 85.5(6), P3–Fe1–P4 84.34(5), C42–Fe1–P1 87.8(6), P3–Fe1–P1 102.99(5), P4–Fe1–P1 172.48(6), C42–Fe1–P2 95.6(7), P3–Fe1–P2 72.60(5), P4–Fe1–P2 98.21(5), P1–Fe1–P2 85.78(5).

hexacoordinated iron with the two *cis* positions occupied by molecules of acetonitrile as shown by crystal structure analysis of $[\text{Fe}(\text{DPPEPM})(\text{CH}_3\text{CN})_2](\text{OTf})_2$ (**4**). In this structure, four phosphorus atoms and two acetonitrile molecules are coordinated to iron(II) in a *cis-α* geometry. The terminal Fe–P bonds are again somewhat longer than internal Fe–P bonds, similar to the trend observed with compounds **2** and **3**, but in general, the average Fe–P bond lengths are not significantly different from those in other iron complexes of neutral phosphine ligands.^{43–45}

The $^{31}\text{P}\{^1\text{H}\}$ NMR spectrum of **4** in CD_2Cl_2 solution shows two pseudo-triplets at 42.8 and 69.7 ppm associated with two different types of phosphorus atoms in the κ^4 -bound DPPEPM. The ^1H NMR (CD_2Cl_2) spectrum exhibits five well-separated broad peaks of equal intensities assigned to coordinated DPPEPM, and a singlet at 1.20 ppm associated with coordinated acetonitrile, Table 1. Free triflate anions exhibit a sharp singlet at –77 ppm in ^{19}F NMR, and the C–F stretch at $\nu = 1209\text{ cm}^{-1}$ in the IR spectrum (KBr). All of the NMR data identify the solution species as κ^4 -coordinated, in contrast to the κ^3 mode observed in solution for the dichloro and dibromo complexes in CD_2Cl_2 . However, the ^{31}P NMR spectrum of **1** in acetonitrile- d_3 (δ 42 and 72) was similar to the $^{31}\text{P}\{^1\text{H}\}$ NMR spectrum of **4** suggesting that the chloride ligands are substituted by acetonitrile.

Substitution Reactions with CO. The reaction of **1** with excess CO in methanol generated $[\text{Fe}\{\text{DPPEPM}\}(\text{CO})\text{Cl}]\text{Cl}$ (**5**) in which one of the original chloride ions was replaced by CO, eq 3. The $^{31}\text{P}\{^1\text{H}\}$ NMR spectrum of **5** exhibits four sets of signals, each consisting of eight lines (ddd). This pattern is

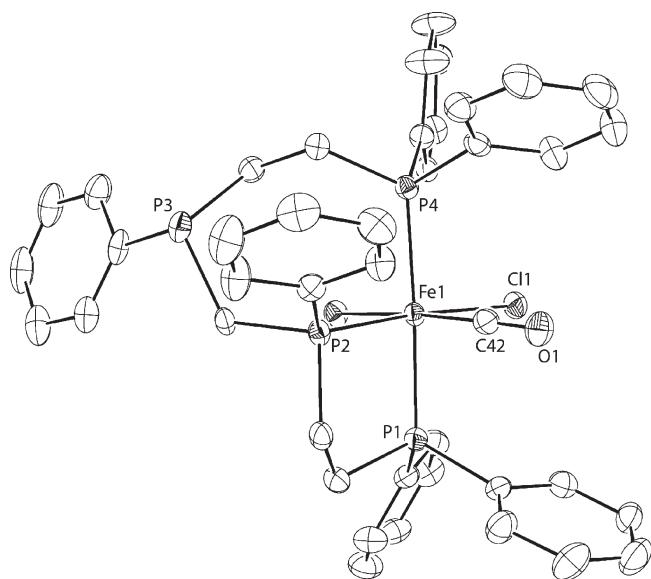
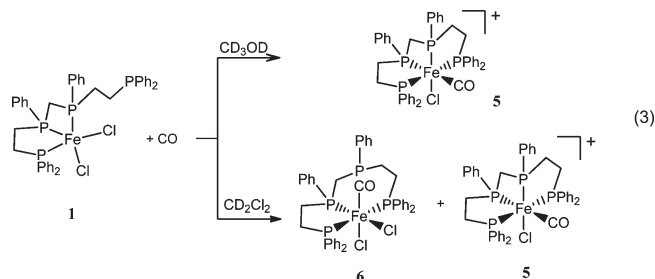


Figure 4. ORTEP drawing of $[\text{Fe}(\kappa^3\text{-DPPEPM})(\text{CO})\text{Cl}_2]$ (**6**). Thermal ellipsoids are drawn at 35% probability level. Hydrogen atoms are omitted for clarity. Selected bond lengths [Å] and angles [deg]: Fe1–C42 1.751(3), Fe1–P2 2.2436(8), Fe–P1 2.2804(8), Fe1–P4 2.2928(8), Fe1–Cl2 2.3329(7), Fe1–Cl1 2.3716(8), P1–C1 1.822(3), C42–Fe1–P2 93.62(9), C42–Fe1–P1 89.86(9), P2–Fe1–P1 86.74(3), C42–Fe1–P4 93.79(9), P2–Fe1–P4 92.83(3), P1–Fe1–P4 176.35(3), C42–Fe1–Cl2 172.32(9), P2–Fe1–Cl2 92.35(3), P1–Fe1–Cl2 85.66(3), P4–Fe1–Cl2 90.73(3), C42–Fe1–Cl1 81.81(9), P2–Fe1–Cl1 174.09(3), P1–Fe1–Cl1 89.50(3), P4–Fe1–Cl1 91.20(3), Cl2–Fe1–Cl1 91.91(3).

consistent with a κ^4 coordination of four nonequivalent phosphorus atoms, as in the structure shown in Figure 3. A large trans coupling of 117 Hz in the ^{31}P spectrum between a cis pair of internal phosphorus atoms is likely due to a stronger coupling through both the iron atom and the carbon atom of the methylene group or due to unusually small P–Fe–P angle of 72.6° . A similar cis iron complex of κ^4 -eHTP ligand exhibits a similar NMR spectrum with a large cis coupling constant.³⁵ The internal phosphine ligands are trans to Cl and CO and might be used to assess the relative contributions of ligand structure and trans influence on the geometry of (DPPEPM)Fe(II) compounds. Indeed, the Fe–P(internal) distances are similar to the Fe–P(external) distances in **5**. However, the chloride and carbonyl ligands are disordered over the two coordination sites limiting the interpretations of the structural data for **5**.



The same reaction in CD_2Cl_2 generated a mixture of **5** and a comparable amount of another complex that was identified as $(\kappa^3\text{-DPPEPM})\text{FeCl}_2(\text{CO})$ (**6**) by crystal structure analysis, Figure 4. In addition to the four resonances characteristic of **5** (and shifted in CD_2Cl_2 to 28.4, 53.2, 63.7, and 87.2 ppm), the

$^{31}\text{P}\{^1\text{H}\}$ NMR spectrum in CD_2Cl_2 exhibits three new resonances at 20.9, 55.3, and 77.2 ppm assigned to coordinated phosphorus atoms. The signal corresponding to the uncoordinated phosphorus at -11.5 ppm is very broad suggesting fast relaxation, caused perhaps by traces of free iron(II) in the sample. Signals corresponding to dangling phosphorus have been shown to disappear upon addition of even trace amounts of FeCl_2 in related complexes.³⁵

Interestingly, the coordination of CO to **1** in CH_2Cl_2 was accompanied by isomerization from 1,4,6- P_3 coordination of DPPEPM to the iron center into a 1,4,9- P_3 bonding mode. Both external phosphorus atoms in the product (**6**) are coordinated, but one of the internal phosphorus atoms is dissociated from the metal. Although the internal dialkylphenylphosphino group is a stronger donor than the external alkylphenylphosphines, the cleavage of an Fe–P(internal) bond in a hexacoordinated complex appears favorable as it should relieve the strain in the bound ligand better than the cleavage of an Fe–P(external) bond would. In the cationic product, **5**, all four phosphorus atoms are coordinated to the metal. The substitution of chloride by CO appears to be more facile in methanol where **5** was the sole observed product. The greater polarity of this solvent should facilitate reactions that proceed through a polar transition state, such as that expected for the dissociation of chloride from **1**.

The apparent partial dissociation and isomerization of coordinated DPPEPM induced by the strain in ligand backbone is one of the features that may make these complexes catalytically active in appropriate reactions. The ability of the catalyst to bind the substrate and release products while preserving its own overall structural integrity is one of the basic and most essential requirements in catalytic chemistry.

CONCLUSIONS

All of the iron complexes of DPPEPM in this work, as well as ruthenium example, exhibit α (folded) geometry. In solid complexes **2**, **3**, **4**, and **5**, the ligand DPPEPM is coordinated in a κ^4 mode and bound in a cis- α configuration. To the best of our knowledge, these are first monometallic, κ^4 complexes of DPPEPM ever reported. Typically, these types of ligands either bind with lower denticity, κ^2 or κ^3 , or form bimetallic complexes,^{32,34} although a κ^4 Rh(III) complex of the related $\text{Et}_2\text{PCH}_2\text{CH}_2\text{P}(\text{Ph})\text{CH}_2\text{P}(\text{Ph})\text{CH}_2\text{CH}_2\text{P}(\text{Et})_2$ has been prepared.³²

In CD_2Cl_2 solutions, one of the Fe–PPh₂(external) bonds in the halo complexes **1** and **2** and in chloro carbonyl complex **6** is cleaved to reduce the denticity of DPPEPM to three. Also, complexes **1** and **2** appear to be present in solution in more than one form as shown by ^1H and ^{31}P NMR in THF and CH_2Cl_2 . Moreover, the two chlorides in **1** are labile as shown by the appearance of the bis-acetonitrile complex **4** upon dissolution of **1** in CH_3CN , Table 1. The apparent kinetic lability of individual sites, combined with the retention of structural integrity of the molecule is an essential feature to be exploited in future design of DPPEPM-based catalysts.

The dicationic bis-acetonitrile complex **4** retains the η^4 ligand binding mode even in solution, as does the singly charged chloro carbonyl complex **5** in methanol and in CD_2Cl_2 . The fine interplay between the overall charge, solvent polarity, and ligand hapticity is another feature that should allow fine-tuning of the potential catalytic activity of these complexes. Even the net outcome of the reaction with CO can be altered by the change

of solvent,⁴⁶ as shown in eq 3. One should expect similar sensitivity to reaction conditions with other substrates.

■ ASSOCIATED CONTENT

S Supporting Information. Figures S1–S9. This information is available free of charge via the Internet at <http://pubs.acs.org>.

■ AUTHOR INFORMATION

Corresponding Author

*E-mail: pvp@iastate.edu (O.P.); bakac@ameslab.gov (A.B.); sadow@iastate.edu (A.S.).

■ ACKNOWLEDGMENT

The support for this project from the Iowa Energy Center (B.J., A.S., A.B., A.E.) and the U.S. Department of Energy, Office of Basic Energy Sciences, Division of Chemical Sciences, Geosciences, and Biosciences through the Ames Laboratory (O.P.) and is gratefully acknowledged. The Ames Laboratory is operated for the U.S. Department of Energy by Iowa State University under Contract No. DE-AC02-07CH11358. The work was carried out in the facilities of the Ames Laboratory and the Chemistry Department at Iowa State University.

■ REFERENCES

- (1) Churchill, D.; Shin, J. H.; Hascall, T.; Hahn, J. M.; Bridgewater, B. M.; Parkin, G. *Organometallics* **1999**, *18*, 2403.
- (2) Lee, H.; Desrosiers, P. J.; Guzei, I.; Rheingold, A. L.; Parkin, G. J. *Am. Chem. Soc.* **1998**, *120*, 3255.
- (3) Shin, J. H.; Parkin, G. *Chem. Commun.* **1999**, 887.
- (4) Carpentier, J.-F.; Maryin, V. P.; Luci, J.; Jordan, R. F. *J. Am. Chem. Soc.* **2001**, *123*, 898.
- (5) Kristian, K. E.; Iimura, M.; Cummings, S. A.; Norton, J. R.; Janak, K. E.; Pang, K. *Organometallics* **2008**, *28*, 493.
- (6) Shapiro, P. J.; Bunel, E.; Schaefer, W. P.; Bercaw, J. E. *Organometallics* **1990**, *9*, 867.
- (7) Shapiro, P. J.; Cotter, W. D.; Schaefer, W. P.; Labinger, J. A.; Bercaw, J. E. *J. Am. Chem. Soc.* **1994**, *116*, 4623.
- (8) Stubbert, B. D.; Marks, T. J. *J. Am. Chem. Soc.* **2007**, *129*, 4253.
- (9) Tian, S.; Arredondo, V. M.; Stern, C. L.; Marks, T. J. *Organometallics* **1999**, *18*, 2568.
- (10) Boncella, J. M.; Green, M. L. H.; O'Hare, D. J. *Chem. Soc., Chem. Commun.* **1986**, 618.
- (11) McNeill, K.; Andersen, R. A.; Bergman, R. G. *J. Am. Chem. Soc.* **1997**, *119*, 11244.
- (12) Peters, J. C.; Feldman, J. D.; Tilley, T. D. *J. Am. Chem. Soc.* **1999**, *121*, 9871.
- (13) Betley, T. A.; Peters, J. C. *Inorg. Chem.* **2003**, *42*, 5074.
- (14) Betley, T. A.; Peters, J. C. *J. Am. Chem. Soc.* **2004**, *126*, 6252.
- (15) Bianchini, C.; Peruzzini, M.; Zanobini, F. *J. Organomet. Chem.* **1988**, *354*, C19.
- (16) Bianchini, C.; Perez, P. J.; Peruzzini, M.; Zanobini, F.; Vacca, A. *Inorg. Chem.* **1991**, *30*, 279.
- (17) Antberg, M.; Dahlenburg, L. *Inorg. Chim. Acta* **1985**, *104*, 51.
- (18) Bampas, N.; Field, L. D. *Inorg. Chem.* **1990**, *29*, 587.
- (19) Bampas, N.; Field, L. D.; Messerle, B. A. *Organometallics* **1993**, *12*, 2529.
- (20) von Zelewsky, A. *Stereochemistry of Coordination Compounds*; Wiley: Chichester, U.K., 1996.
- (21) Bautista, M. T.; Earl, K. A.; Maltby, P. A.; Morris, R. H.; Schweitzer, C. T. *Can. J. Chem.* **1994**, *72*, 547.
- (22) Ghilardi, C. A.; Midollini, S.; Sacconi, L.; Stoppioni, P. *J. Organomet. Chem.* **1981**, *205*, 193.
- (23) Girolami, G. S.; Wilkinson, G.; Galas, A. M. R.; Thornton-Pett, M.; Hursthouse, M. B. *J. Chem. Soc., Dalton Trans.* **1985**, 1339.
- (24) Hills, A.; Hughes, D. L.; Jimenez-Tenorio, M.; Leigh, G. J.; Rowley, A. T. *J. Chem. Soc., Dalton Trans.* **1993**, 3041.
- (25) Miller, W. K.; Gilbertson, J. D.; Leiva-Paredes, C.; Bernatis, P. R.; Weakley, T. J. R.; Lyon, D. K.; Tyler, D. R. *Inorg. Chem.* **2002**, *41*, 5453.
- (26) Field, L. D.; Thomas, I. P.; Hambley, T. W.; Turner, P. *Inorg. Chem.* **1998**, *37*, 612.
- (27) Baker, M. V.; Field, L. D. *J. Am. Chem. Soc.* **1987**, *109*, 2825.
- (28) Baker, M. V.; Field, L. D. *J. Am. Chem. Soc.* **1986**, *108*, 7433.
- (29) Bautista, M. T.; Earl, K. A.; Maltby, P. A.; Morris, R. H. *J. Am. Chem. Soc.* **1988**, *110*, 4056.
- (30) Brown, J. M.; Canning, L. R. *J. Organomet. Chem.* **1984**, *267*, 179.
- (31) Laneman, S. A.; Fronczek, F. R.; Stanley, G. G. *Inorg. Chem.* **1989**, *28*, 1872.
- (32) Hunt, C. J.; Fronczek, F. R.; Billodeaux, D. R.; Stanley, G. G. *Inorg. Chem.* **2001**, *40*, 5192.
- (33) Nair, P.; Anderson, G. K.; Rath, N. P. *Inorg. Chem. Commun.* **2002**, *5*, 653.
- (34) Nair, P.; White, C. P.; Anderson, G. K.; Rath, N. P. *J. Organomet. Chem.* **2006**, *691*, 529.
- (35) Askham, F. R.; Saum, S. E.; Stanley, G. G. *Organometallics* **1987**, *6*, 1370.
- (36) Gilbertson, J. D.; Szymczak, N. K.; Tyler, D. R. *J. Am. Chem. Soc.* **2005**, *127*, 10184.
- (37) Hagen, K. S. *Inorg. Chem.* **2000**, *39*, 5867.
- (38) Albers, M. O.; Ashworth, T. V.; Oosthuizen, H. E.; Singleton, E. *Inorg. Synth.* **1989**, *26*, 68.
- (39) Hallman, P. S.; Stephenson, T. A.; Wilkinson, G. *Inorg. Synth.* **1970**, *12*, 237.
- (40) Jee, J.-E.; Pestovsky, O.; Bakac, A. *Dalton Trans.* **2010**, *39*, 11636.
- (41) Garrou, P. E. *Chem. Rev.* **1981**, *81*, 229.
- (42) Burrows, A. D.; Dodds, D.; Kirk, A. S.; Lowe, J. P.; Mahon, M. F.; Warren, J. E.; Whittlesey, M. K. *Dalton Trans.* **2007**, 570.
- (43) Allen, O. R.; Dalgarno, S. J.; Field, L. D. *Organometallics* **2008**, *27*, 3328.
- (44) Field, L. D.; Messerle, B. A.; Smernik, R. J.; Hambley, T. W.; Turner, P. *Inorg. Chem.* **1997**, *36*, 2884.
- (45) George, A. V.; Field, L. D.; Malouf, E. Y.; McQueen, A. E. D.; Pike, S. R.; Purches, G. R.; Hambley, T. W.; Buys, I. E.; White, A. H.; Hockless, D. C. R.; Skelton, B. W. *J. Organomet. Chem.* **1997**, *538*, 101.
- (46) Burrows, A. D.; Harrington, R. W.; Kirk, A. S.; Mahon, M. F.; Marken, F.; Warren, J. E.; Whittlesey, M. K. *Inorg. Chem.* **2009**, *48*, 9924.